Journal of Sound and Vibration (1999) **228**(2), 377–396
Article No. jsvi.1999.2416, available online at http://www.idealibrary.com on IDEAL®

MOVING FORCES IDENTIFICATION ON A MULTI-SPAN CONTINUOUS BRIDGE

X. Q. ZHU AND S. S. LAW

Civil and Structural Engineering Department, The Hong Kong Polytechnic University, Hunghom, Kowloon, Hong Kong

(*Received* 21 *December* 1998, *and in final form* 26 *May* 1999)

A continuous bridge is modelled as a multi-span continuous Timoshenko beam with non-uniform cross-section. The vibration behaviour of this beam subjected to moving loads is analyzed by Hamilton's principle with the intermediate point constraints represented by very stiff linear springs. A method based on the modal superposition and optimization technique is developed to identify the moving forces in the time domain. The damped least-squares method is used in the identification to provide bounds to the results. The errors in the moving force identification are discussed in the paper. Both computation simulations and laboratory tests show that the method is effective for identifying the moving loads using different combinations of measured responses

1. INTRODUCTION

The problem of bridge vibration caused by moving vehicles has been studied for many years. The research mainly focused on the effect of different parameters such as suspension systems, road surface roughness, bridge parameters, vehicle parameters and damping on bridge responses. The bridge is modelled in a variety of ways using the finite element method. The vehicle is also modelled with different degrees of complexity. However, no work is known to the authors which investigates the real interaction forces between the vehicle and the bridge deck. A direct way to study these forces is to use an instrumented vehicle to measure them. Whittemore *et al.* [1] and Cantieni [2] have given summaries on some of these systems which are subjected to bias. These all indicate the need to develop a method to measure the dynamic interaction forces using an unbiased random sample of vehicles.

Law *et al.* [3] models the structure and forces with a set of second order differential equations. The forces are represented as step functions in a small time interval. These equations of motions are then expressed in the modal co-ordinates, and these uncoupled equations are solved by convolution in the time domain. The forces are then identified using the modal superposition principle. Law *et al.* [4] performs Fourier transformation on the equations of motions, which are expressed in modal co-ordinates. The Fourier transforms of the responses and the forces are

0022-460X/99/470377 + 20 $30.00/0

related in the frequency domain, and the time histories of the forces are found directly by the least-squares method. Later, Chan *et al.* [5] identify the forces completely in the modal co-ordinates. Measured displacements are converted into modal displacements with an assumed shape function. The modal velocities and accelerations are then obtained by differentiation. The forces are then identified solving the uncoupled equations of motions in modal co-ordinates. Law and Fang [6] have also reported a state estimation approach in which the state-space formulation of the dynamic system is solved using dynamic programming with minimization of the errors between the measured and the reconstructed responses from the identified moving forces.

All the above approaches are based on the Bernoulli–Euler beam theory, and they refer to the interaction with a simply supported beam. But there are a lot of multi-span continuous bridges of large cross-section, and the effect of variation of the cross-sectional dimensions on the dynamic properties cannot be neglected. The effect of rotatory inertia and of shear deformation must be considered.

Lee [7] and later Zheng *et al.* [8] have studied the vibration behaviour of a multi-span continuous bridge modelled as a multi-span non-uniform continuous Bernoulli–Euler beam under a set of moving loads using different assumed mode shapes. Wu and Dai [9], Henchi and Fafard [10] used the same Bernoulli–Euler beam and the finite element transfer matrix approach. Wang [11] and Wang and Lin [12] have studied the vibration of a continuous beam and a T-frame bridge deck using the Timoshenko beam model. In the present work, the vibration behaviour of the multi-span non-uniform Timoshenko beam subjected to a set of moving loads is analyzed based on Hamilton's principle with the intermediate point constraints represented by very stiff linear springs. The loads can take up any initial positions on the beam. A method to identify these moving forces in the time domain is then developed based on the modal superposition and optimization technique. Since the inverse problem always produces unbounded results [13] due to the non-continuity of the dependence of the results with the measured responses, a damped least-squares method is used to smooth out the large variations in the identified forces. Both single and two forces moving on the beam are identified using displacement or strain measurements at several distributed points on the beam. Computation simulations and laboratory results show that the method is effective and robust, and acceptable results can be obtained from strain and displacement measurements.

2. THEORY OF MOVING FORCE IDENTIFICATION

2.1. VIBRATION ANALYSIS OF A MULTI-SPAN BRIDGE

Figure 1 shows a continuous Timoshenko beam with $(Q-1)$ intermediate point supports under N_f number of moving loads. The beam is constrained at these supports. The loads $P_i(t)$ $(i = 1, 2, \ldots, N_f)$ are moving as a group at a prescribed velocity v along the axial direction of the beam from left to right. v is assumed constant in this study. The load locations are described by $\hat{x}_i(t)$ with $\hat{x}_i(t) = \hat{x}_{i0} + vt$ where $\hat{x}_{i0}$ is the initial location of the load $P_i(t)$. The bending

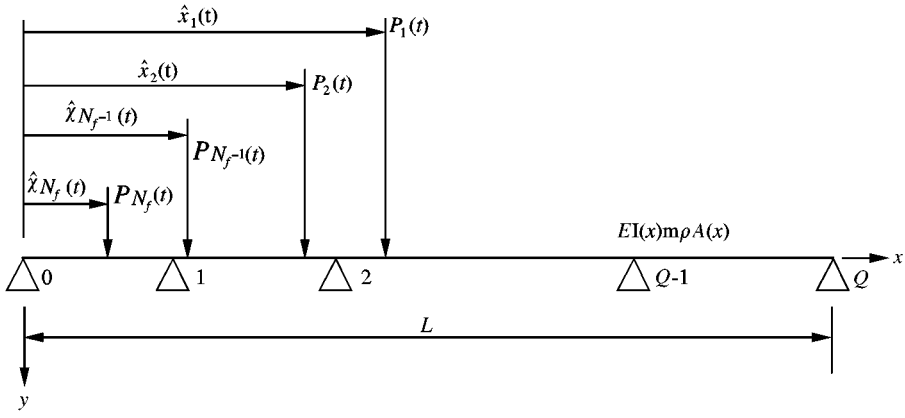

Figure 1. A continuous beam with $(Q-1)$ intermediate point supports under N_f moving forces.

moment and the transverse shear force of the beam are given as

$$M(x) = EI(x)\frac{\partial \psi(x,t)}{\partial x},$$
$$V(x) = \kappa GA(x)\left[\frac{\partial y(x,t)}{\partial x} - \psi(x,t)\right], \tag{1}$$

where G is the shear modulus of the beam material and $A(x)$ is the cross-sectional area, E is the Young's modulus, $I(x)$ is the moment of the inertia of the beam cross-section, κ is the shear coefficient, $y(x,t)$ is the transverse displacement function of the beam, $\psi(x,t)$ is the angle of rotation at a cross-section.

The kinetic energy T of the beam, the strain energy U_e, the potential energy due to point constraints U_Q, and the work done W due to the moving loads can be written for the Timoshenko beam as follows:

$$T = \frac{1}{2}\int_0^L \rho A(x)\left[\left(\frac{\partial y(x,t)}{\partial t}\right)^2 + \gamma^2(x)\left(\frac{\partial \psi(x,t)}{\partial t}\right)^2\right]\mathrm{d}x,$$
$$U_e = \frac{1}{2}\int_0^L \left[EI(x)\left(\frac{\partial \psi(x,t)}{\partial x}\right)^2 + \kappa GA(x)\left(\frac{\partial y(x,t)}{\partial x} - \psi(x,t)\right)^2\right]\mathrm{d}x,$$
$$U_Q = \frac{1}{2}k\sum_{i=1}^{Q-1} y(x_i,t)^2,$$
$$W = \int_0^L \sum_{i=1}^{N_f} \delta(x - \hat{x}_i(t))P_i(t)y(x,t)\,\mathrm{d}x, \tag{2}$$

where ρ is the mass density of the material of the beam; $x_i (i = 0, 1, 2, \ldots, Q)$ are co-ordinate of the intermediate point supports and end supports and $\delta(t)$ is the Dirac delta function. $\gamma(x)$ is the radius of gyration of the beam cross-section. k is the stiffness of the point constraints. Expressing the vibration responses of the beam

$y(x, t)$ and $\psi(x, t)$ in modal co-ordinates,

$$\begin{aligned} y(x,t) &= \sum_{i=1}^{n} q_i(t)\, Y_i(x) \\ \psi(x,t) &= \sum_{i=1}^{n} q_i(t)\, \phi_i(x) \end{aligned} \qquad (i = 1, 2, \ldots, n), \tag{3}$$

where $Y_i(x)$, $\phi_i(x)$ are the assumed vibration modes that satisfy the boundary conditions and $q_i(t)$ is the generalized co-ordinate.

Substituting equation (3) into equation (2), we obtain

$$\begin{aligned} T &= \frac{1}{2}\int_0^L \rho A(x)\left[\sum_{i=1}^{n} \dot{q}_i(t)\, Y_i(x) \sum_{j=1}^{n} \dot{q}_j(t)\, Y_j(x) + \gamma^2(x) \sum_{i=1}^{n}\sum_{j=1}^{n} \dot{q}_i(t)\phi_i(x)\dot{q}_j(t)\phi_j(x)\right] \mathrm{d}x \\ &= \frac{1}{2}\sum_{i=1}^{n}\sum_{j=1}^{n} \dot{q}_i(t) m_{ij} \dot{q}_j(t), \\ U_e &= \frac{1}{2}\int_0^L \left[EI(x) \sum_{i=1}^{n} q_i(t)\phi_i'(x) \sum_{j=1}^{n} q_i(x)\phi_j'(x) \right. \\ &\quad \left. + \kappa GA(x)\left(\sum_{i=1}^{n} q_i(t)\, Y_i'(x) - \sum_{i=1}^{n} q_i(t)\phi_i(x)\right)\left(\sum_{j=1}^{n} q_j(t)\, Y_j'(x) - \sum_{j=1}^{n} q_j(t)\phi_j(x)\right)\right] \mathrm{d}x \\ &= \frac{1}{2}\sum_{i=1}^{n}\sum_{j=1}^{n} q_i(t) k_{ij}' q_j(t), \\ U_Q &= \frac{1}{2} k \sum_{s=1}^{Q-1}\sum_{i=1}^{n} q_i(t)\, Y_i(x_s) \sum_{j=1}^{n} q_j(t)\, Y_j(x_s) = \frac{1}{2}\sum_{i=1}^{n}\sum_{j=1}^{n} q_i(t) k_{ij}'' q_j(t), \\ W &= \int_0^L \sum_{i=1}^{N_f} \delta(x - \hat{x}_j(t)) P_j(t) \sum_{i=1}^{n} q_i(t)\, Y_i(x)\, \mathrm{d}x = \sum_{i=1}^{n} q_i(t) f_i(t), \end{aligned} \tag{4}$$

where

$$\begin{aligned} m_{ij} &= \int_0^L \rho A(x)[\, Y_i(x)\, Y_j(x) + \gamma^2(x)\phi_i(x)\phi_j(x)]\, \mathrm{d}x, \\ k_{ij}' &= \int_0^L [EI(x)\phi_i'(x)\phi_j'(x) + \kappa GA(x)(Y_i'(x) - \phi_i(x))(Y_j'(x) - \phi_j(x))]\, \mathrm{d}x \\ k_{ij}'' &= k \sum_{i=1}^{Q-1} Y_i(x_i)\, Y_j(x_i), \\ f_i(t) &= \sum_{i=1}^{N_f} P_l(t)\, Y_i(\hat{x}_l(t)) \quad (i = 1, 2, \ldots, n; j = 1, 2, \ldots, n) \end{aligned} \tag{5}$$

and $\dot{q}_i(t)$ and $\phi_i'(x)$ denote the first derivatives of $q_i(t)$ and $\phi_i(x)$; m_{ij} is the generalized mass, and $f_i(t)$ is the generalized force. Let $k_{ij} = k_{ij}' + k_{ij}''$, k_{ij} be the

generalized stiffness. The Lagrange equation may be written as follows:

$$\frac{\mathrm{d}}{\mathrm{d}t}\left(\frac{\partial T}{\partial \dot{q}}\right) - \frac{\partial T}{\partial q} + \frac{\partial U}{\partial q} - \frac{\partial W_c}{\partial q} = \frac{\partial W}{\partial q}, \qquad W_c = -q^{\mathrm{T}} C \dot{q}, \tag{6}$$

where W_c is the work due to the viscous damping in the beam. Substituting equation (4) into equation (6), the equation can be written as

$$\sum_{j=1}^{n} m_{ij}\ddot{q}_j(t) + \sum_{j=1}^{n} c_{ij}\dot{q}_j(t) + \sum_{j=1}^{n} k_{ij}q_j(t) = f_i(t), \quad (i = 1, 2, \ldots, n) \tag{7}$$

and in matrix form as

$$M\ddot{q}(t) + C\dot{q}(t) + Kq(t) = F(t), \tag{8}$$

where

$$\begin{aligned} M &= \{m_{ij}, i = 1, 2, \ldots, n; j = 1, 2, \ldots, n\}, \\ K &= \{k_{ij}, i = 1, 2, \ldots, n; j = 1, 2, \ldots, n\}, \\ C &= \{c_{ij}, i = 1, 2, \ldots, n; j = 1, 2, \ldots, n\}, \\ q(t) &= \{q_1(t), q_2(t), \ldots, q_n(t)\}^{\mathrm{T}}, \\ F(t) &= \{f_1(t), f_2(t), \ldots, f_n(t)\}^{\mathrm{T}}. \end{aligned} \tag{9}$$

2.2. THE ASSUMED VIBRATION MODES

The general form of the vibration mode for a uniform Timoshenko beam can be written as follows:

$$\begin{aligned} Y(x) &= D_1\cos(\alpha x) + D_2\sin(\alpha x) + D_3\cosh(\beta x) + D_4\sinh(\beta x), \\ \psi(x) &= D'_1\cos(\alpha x) + D'_2\sin(\alpha x) + D'_3\cosh(\beta x) + D'_4\sinh(\beta x), \end{aligned} \tag{10}$$

where D_1, D_2, D_3, D_4, D'_1, D'_2, D'_3, D'_4, are constants, and α, β are frequency parameters. The vibration modes of a Timoshenko beam with simply supported ends are obtained as follows according to Huang [14]:

$$\begin{aligned} Y_i(x) &= B_i \sin\left(\frac{\mathrm{i}\pi x}{L}\right), \\ \phi_i(x) &= \cos\left(\frac{\mathrm{i}\pi x}{L}\right), \end{aligned} \tag{11}$$

where

$$\begin{aligned} B_i &= \frac{\mathrm{i}\pi L}{(\mathrm{i}\pi)^2 - b_i^2 s^2}, \quad s^2 = \frac{EI}{\kappa AGL^2}, \quad r^2 = \frac{1}{AL}, \\ b_i^2 &= \frac{1 + (\mathrm{i}\pi)^2(r^2 + s^2) - \sqrt{(1 + (\mathrm{i}\pi)^2(r^2 + s^2)^2)^2 - 4(\mathrm{i}\pi)^4 r^2 s^2}}{2r^2 s^2}. \end{aligned} \tag{12}$$

2.3. MOVING FORCE IDENTIFICATION FROM DISPLACEMENTS

Express $y(x_s, t)$ in modal co-ordinates,

$$y(x_s, t) = \sum_{i=1}^{n} Y_i(x_s) q_i(t) \quad (s = 1, 2, \ldots, N_d), \tag{13}$$

where N_d is the number of measurement locations; $\{y(x_s, t), s = 1, 2, \ldots, N_d\}$ are the displacements at x_s. Equation (13) can be written as

$$\{y\}_{N_d \times 1} = [Y]_{N_d \times n} \{q\}_{n \times 1}, \tag{14}$$

where $\{y\}_{N_d \times 1}$ is the vector of displacements at N_d measurement locations. The vector of generalized co-ordinates can then be written using the well-known least-squares pseudo-inverse

$$\{q\}_{n \times 1} = ([Y]^{\mathrm{T}}_{n \times N_d} [Y]_{N_d \times n})^{-1} [Y]^{\mathrm{T}}_{n \times N_d} \{y\}_{N_d \times 1}. \tag{15}$$

The modal velocity and acceleration are obtained by differentiation, and they are substituted into equation (8) to get

$$\{F\}_{n \times 1} = M_{n \times n} \{\ddot{q}\}_{n \times 1} + C_{n \times n} \{\dot{q}\}_{n \times l} + K_{n \times n} \{q\}_{n \times 1}. \tag{16}$$

The vector of generalized forces $\{F\}$ can also be found from equation (5) as

$$\{F\}_{n \times l} = [B]_{n \times N_f} \{P\}_{N_f \times l}, \tag{17}$$

where $\{P\}_{N_f \times 1}$ are the moving forces on the beam, and

$$[B]_{n \times N_f} = \begin{bmatrix} Y_1(\hat{x}_1(t)) & Y_1(\hat{x}_2(t)) & \cdots & Y_1(\hat{x}_{N_f}(t)) \\ Y_2(\hat{x}_1(t)) & Y_2(\hat{x}_2(t)) & \cdots & Y_2(\hat{x}_{N_f}(t)) \\ \vdots & \vdots & \vdots & \vdots \\ Y_n(\hat{x}_1(t)) & Y_n(\hat{x}_2(t)) & \cdots & Y_n(\hat{x}_{N_f}(t)) \end{bmatrix}_{n \times N_f} \tag{18}$$

By the simple least-squares method (LS), the moving force can be calculated directly from

$$\{P\}_{N_f \times 1} = ([B]^{\mathrm{T}}_{N_f \times n} [B]_{n \times N_f})^{-1} [B]^{\mathrm{T}}_{N_f \times n} \{F\}_{n \times 1}. \tag{19}$$

But since the identified forces $\{P\}$ are not continuous functions of the generalized forces $\{F\}$, are variations in the results would be obtained by the simple least-squares method. In order to have bounds on the ill-conditioned forces, the damped least-squares method (DLS) [15] is used and singular-value

decomposition is used in the pseudo-inverse calculation. Equation (19) can be written in the following form using the DLS method:

$$\{P\}_{N_f\times 1} = ([B]^{\mathrm{T}}_{N_f\times n}[B]_{n\times N_f} + \lambda I)^{-1}[B]^{\mathrm{T}}_{N_f\times n}\{F\}_{n\times 1}, \tag{20}$$

where λ is the non-negative damping coefficient governing the participation of the least-squares error in the solution. The solution of equation (20) is equivalent to minimizing the function

$$J(\{P\}, \lambda) = \|[B]\{P\} - \{F\}\|^2 + \lambda\|\{P\}\|^2 \tag{21}$$

and the second term in equation (21) provides bounds to the solution. When λ approaches zero, the estimated vector $\{P\}$ approaches the solution obtained from the least-squares method. In practice, the expected value of λ is not known, and there is no guideline to select the optimal value of λ. Both the discrepancy principle [16] and the generalized cross-validation method [17] cannot be used here. In the simulation studies described below, the error between the true and the estimated forces is minimized [18] for a specific range of λ. In the experimental identification of the forces, the error in the identified forces between successive computation with an increment of λ is minimized instead.

The identified forces are obtained through the following computations: The mode shapes $Y_i(t)$ are computed from equation (11). The generalized co-ordinate $q_i(t)$ is computed from equation (15) with information on the measured displacements $y(x_s, t)$. The derivatives of $\mathbf{q}$ and the system matrices are computed, and the generalized force vector $\mathbf{F}$ is obtained from equation (16). Matrix $\mathbf{B}$ is obtained from equation (18) with information of the normal mode shapes. The non-negative damping coefficient λ is obtained from minimization as discussed in the last paragraph, and then the moving force vector $\mathbf{P}$ is identified from equations (19) and (20) for the least-squares and damped least-squares method.

2.4. MOVING FORCE IDENTIFICATION FROM STRAINS

The strain at the bottom of the beam can be expressed in terms of the generalized co-ordinate as

$$\varepsilon(x_s, t) = -\frac{h}{2}\sum_{i=l}^{n}\phi_i'(x_s)q_i(t) \quad (s = 1, 2, \ldots, N_s), \tag{22}$$

where N_s is the number of measurement points; $\{\varepsilon(x_s, t), s = 1, 2, \ldots, N_s\}$ are the strain at x_s. When written in matrix form,

$$\{\varepsilon\}_{N_s\times 1} = [\phi']_{N_s\times n}\{q\}_{n\times 1}. \tag{23}$$

The vector of generalized co-ordinates $\{q\}_{n\times 1}$ can be similarly calculated as for equation (14):

$$\{q\}_{n\times 1} = ([\phi']^{\mathrm{T}}_{n\times N_s}[\phi']_{N_s\times n})^{-1}[\phi']^{\mathrm{T}}_{n\times N_s}\{\varepsilon\}_{N_s\times 1}. \tag{24}$$

The subsequent identification process would be the same as for the displacements.

2.5. MOVING FORCE IDENTIFICATION FROM BOTH STRAINS DISPLACEMENTS

If the strains and displacements are measured at the same time, both of them can be used in the identification. But the strains and displacements should be scaled by their respective norms to have dimensionless units.

$$\begin{Bmatrix} \dfrac{\varepsilon}{\|\varepsilon\|} \\ \dfrac{y}{\|y\|} \end{Bmatrix}_{(N_s+N_d)\times 1} = \begin{Bmatrix} \dfrac{\phi'}{\|\varepsilon\|} \\ \dfrac{Y}{\|y\|} \end{Bmatrix}_{(N_s+N_d)\times n} \{q\}_{n\times l}, \tag{25}$$

where $\|\cdot\|$ is the norm of the vector.

3. SIMULATION AND RESULTS

3.1. SINGLE FORCE IDENTIFICATION ON A SINGLE SPAN BEAM

A single span simply supported beam with a single force moving on top is studied.

$$f(t) = 40\,000[1 + 0{\cdot}1\sin(10\pi t) + 0{\cdot}05\sin(40\pi t)], \quad N.$$

The parameters of the beam are as follows: $EI = 1{\cdot}274916\times 10^{11}\,\mathrm{N\,m^2}$, $\rho = 7700\,\mathrm{kg\,m^3}$, $\rho A = 12\,000\,\mathrm{kg/m}$, $L = 20\,\mathrm{m}$, $G = 77{\cdot}6^9\,\mathrm{N\,m^2}$. The moving speed is 20 m/s, and the shear coefficient κ is $\frac{5}{6}$. The first three modes of the beam are considered. White noise is added to the calculated displacements to simulate the polluted measurements as follows. 1, 5 and 10 per cent noise levels are studied.

$$y = y_{\mathrm{calculated}}(1 + Ep * N_{oise}), \quad \varepsilon = \varepsilon_{\mathrm{calculated}}(1 + Ep * N_{oise}),$$

where y and ε are the displacement and strain, respectively, E_p is the noise level, N_{oise} is a standard normal distribution vector with zero mean value and unit standard deviation. $y_{\mathrm{calculated}}$ and $\varepsilon_{\mathrm{calculated}}$ are the calculated displacement and strain.

The errors in the identified forces are calculated as

$$Error = \frac{\|P_{identified} - P_{True}\|}{\|P_{True}\|} \times 100\%. \tag{26}$$

TABLE 1

Errors in single force identification (*in per cent*)

Number of vibration modes	Noise level		
	1%	5%	10%
1	16·83	17·31	19·08
2	12·04	12·81	15·24
3	10·36	11·31	14·07
4	9·75	10·80	13·72
5	9·51	10·61	13·61
6	9·16	10·32	13·41
7	9·20	10·38	13·49
8	8·79	10·04	13·25
9	9·54	10·72	13·78
10	9·92	11·05	14·04

TABLE 2

Errors in single force identification (*in per cent*)

Number of measuring points	Noise level		
	1%	5%	10%
1	104·44	104·52	104·78
2	25·30	25·14	25·69
3	9·94	10·32	12·69
4	9·94	10·32	12·88
5	9·94	10·32	12·88

Table 1 shows the errors in single force identification with different number of vibration modes. The responses at ten measurement points evenly distributed along the beam are simulated from the first ten modes. These responses are used in the identification. Table 2 shows the errors in single force identification with different number of measuring points, and the first three modes are used in the simulation. Figure 2 shows the identified results with different number of vibration modes. Displacement responses from the same number of sensors as the vibration modes are used. The sampling frequency is 2·5 times the maximum natural frequency of interest for the above studies.

The following results are obtained in the simulation studies:

(1) The results show that the proposed method and algorithms for one moving force identification are correct. The identified force is very close to the true force.

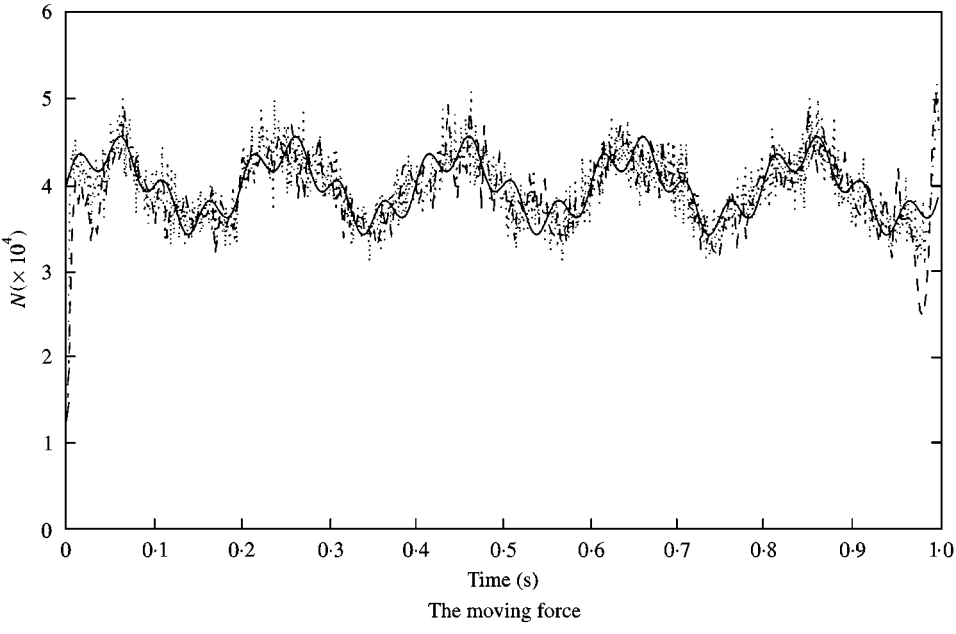

Figure 2. Time histories of identified force in single force simulation: ——, true force; - - - -, from 3 modes; ...., from 6 modes.

(2) When the number of displacement response is not less than the number of vibration modes, the error is small, and it decreases with increase in the number of responses used. This indicates that the number of displacement responses must not be less than the number of the vibration modes used in the identification. The number of displacement responses can be taken to be equal to the number of the vibration modes in the force identification.
(3) The error in the identified force is not sensitive to the noise level in the response measurements used for the identification.
(4) Table 1 shows that the error in the identified force exhibits little change when the number of the vibration modes is larger than 3. This may be due to the fact that the fourth mode is at a frequency of approximately 110 Hz, and the modal response of the beam is small. Additional vibration modes higher than the third mode contain less information on the moving forces. This is supported by Figure 2 where the identified force from both three modes and six modes are very close to the true force except for some variations close to the entry and exit of the force.

3.2. TWO-FORCE IDENTIFICATION ON TWO-SPAN CONTINUOUS BEAM

Again a two-span simply supported beam is considered. The total length is 40 m, and the intermediate support is at the middle of the beam. This support is modelled with a stiff linear spring of stiffness equals to 10^{16} N/m. The parameters of the beam

are the same as that for example one. The two moving forces are

$$f_1(t) = 20\,000[1 + 0{\cdot}1\sin(10\pi t) + 0{\cdot}05\sin(40\pi t)], \quad N,$$
$$f_2(t) = 20\,000[1 - 0{\cdot}1\sin(10\pi t) + 0{\cdot}05\sin(50\pi t)], \quad N,$$

and they are moving at 40 m/s. The distance l_s between the two moving forces is 4 m. Again, the first three modes are used in the calculation. The damping ratio is 0·02 for all the three modes. The sampling frequency is 100 Hz and 110 points are used in the identification. The strain and displacement measurements at the $\frac{1}{8}$, $\frac{1}{4}$ and $\frac{5}{8}$ spans are used with 5 per cent added noise. The identified forces performed by both the LS and DLS methods are shown in Figures 3 and 4 in Tables 3 and 4. The following observations are made:

(1) When the number of measured strains and displacements are not less than the number of vibration modes used in the identification, acceptable results could be obtained. This shows that the proposed method and the algorithm used for two-force identification are correct and they can be used in a practical multi-forces situation.
(2) The magnitude of error remains relatively constant with different noise level. This indicates that the proposed method is not sensitive to noise.
(3) There are impulses in the forces at both the entry and exit of the beam. This discrepancy is found to decrease as the stiffness of the beam is increased in the simulation. This is due to the low sensitivity of the bridge responses to the forces at the beginning and the end of the beam.

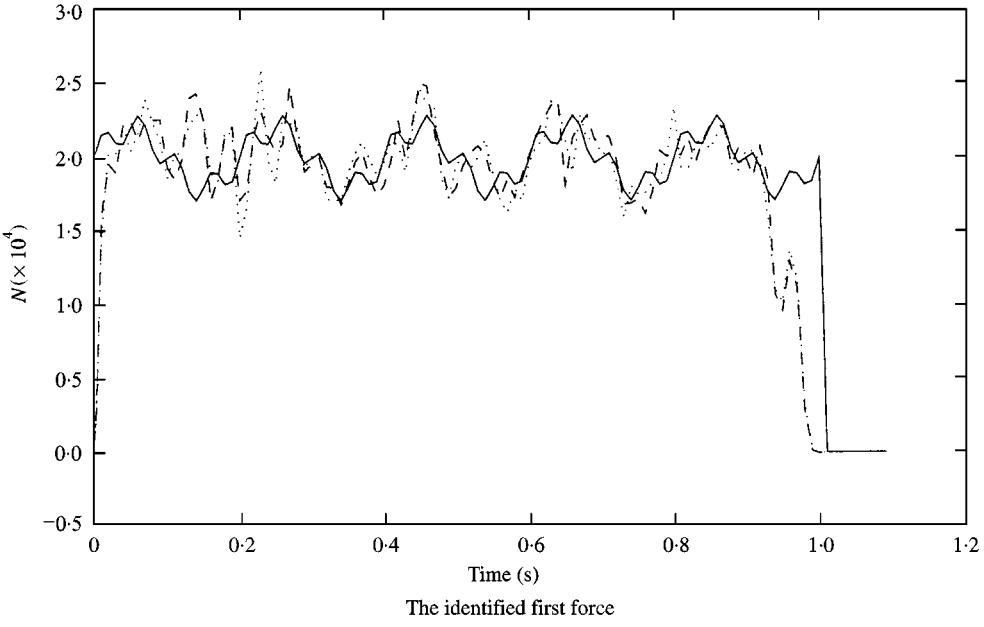

Figure 3. Time histories of identified first force in two forces simulation: ——, true force; - - - -, $\frac{1}{8}$, $\frac{1}{4}$, $\frac{5}{8}$D; ...., $\frac{1}{8}$, $\frac{1}{4}$, $\frac{5}{8}\varepsilon$.

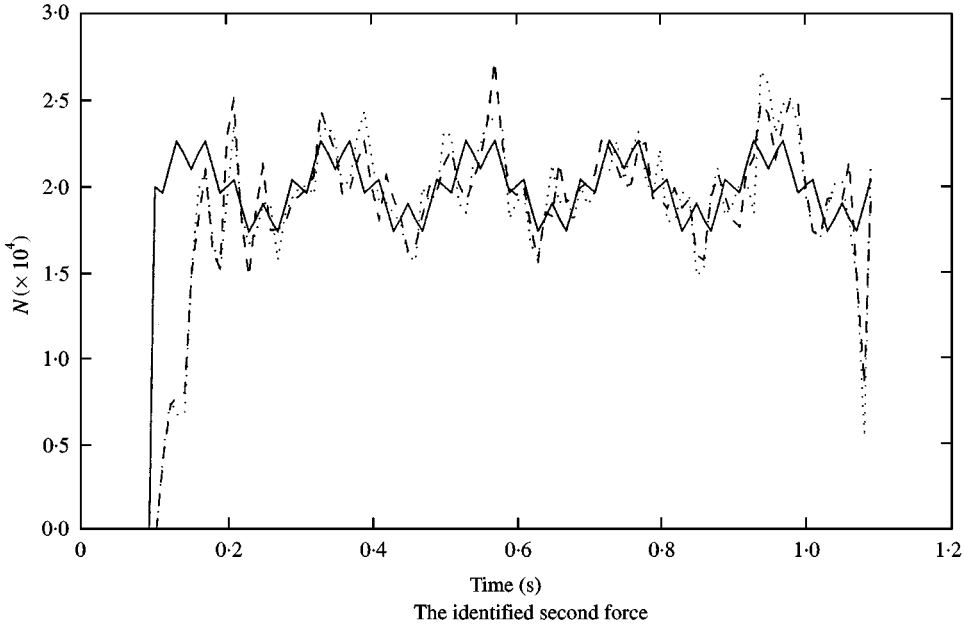

Figure 4. Time histories of identified second force in two forces simulation: ——, true force; - - - -, $\frac{1}{8}$, $\frac{1}{4}$, $\frac{5}{8}$D; ...., $\frac{1}{8}$, $\frac{1}{4}$, $\frac{5}{8}\varepsilon$.

TABLE 3

Errors in two-force identification by LS method (*in per cent*)

Locations and responses	1% error in response		5% error in response		10% error in response	
	First	Second	First	Second	First	Second
1/4D, 3/4D	*	*	*	*	*	*
1/8D, 1/4D, 3/8D	73·10	112·78	75·22	104·47	75·63	105·00
1/8D, 1/4D, 5/8D	72·99	112·76	71·61	117·21	79·28	118·44
1/8D, 1/4D, 3/4D	72·21	111·90	69·70	111·40	78·26	83·34
1/8D, 3/4D, 3/8D	73·37	113·41	71·57	110·92	74·79	107·14
1/8D, 1/8s, 1/4D	72·87	114·25	77·15	116·93	73·31	125·75
1/8D, 1/4D, 1/4s	72·87	113·35	73·52	111·52	78·60	101·82
1/8s, 1/4s, 1/8D	72·80	113·79	73·40	113·60	72·17	118·60
1/8s, 1/4s, 3/8s	72·58	111·67	68·83	111·08	75·83	114·98

Note: * Represents the error in larger than 1000%

(4) The moving forces on a two-span continuous beam can be identified by only the measuring data on one-span using the two-span continuous beam model of the structure.

TABLE 4

Errors in two-force identification by DLS method (in per cent)

Locations and responses	1% error in response		5% error in response		10% error in response	
	First	Second	First	Second	First	Second
1/4D, 3/4D	*	*	*	*	*	*
1/8D, 1/4D, 3/8D	25·72	29·41	25·80	29·78	26·33	30·81
1/8D, 1/4D, 5/8D	25·63	29·31	26·38	29·87	27·38	30·25
1/8D, 1/4D, 3/4D	25·61	29·44	25·64	29·82	27·81	30·01
1/8D, 3/4D, 3/8D	25·75	29·37	26·29	30·30	28·28	31·37
1/8D, 1/8s, 1/4D	25·60	29·35	26·04	29·57	26·83	31·24
1/8D, 1/4D, 1/4s	25·68	29·32	25·66	30·03	28·30	30·06
1/8s, 1/4s, 1/8D	25·75	29·38	25·97	30·06	29·24	30·24
1/8s, 1/4s, 3/8s	25·74	29·33	25·97	29·87	27·28	31·84

Note: * Represents the error in larger than 1000%

(5) The forces identified from the strains are of the same accuracy as those obtained from the displacements. But since the strain measurements can be easily obtained, force identification from the strain measurements would be very convenient and useful.
(6) The error in the identified forces obtained by using LS is larger than that from using DLS. This shows the effectiveness of the damped least-squares method in providing bounds on the ill-conditioned forces with an optimal damping coefficient λ.

4. EXPERIMENT AND RESULTS

The experimental set-up is shown in Figure 5. The main beam, 3678 mm long with a 100 mm × 25 mm uniform cross-section, is simply supported. A U-shaped aluminium section is glued to the upper surface of the beams as a direction guide for the car. The model car is pulled along the guide by a string wound around the drive wheel of an electric motor. Seven photoelectric sensors are evenly mounted onto the beam to measure and monitor the moving speed of the car. They are located on the beam at an interval of 0·776 m to check on the uniformity of the speed. Seven strain gauges are evenly located on the under system of the beam at one-eighth span to measure the responses of the beam. An eight-channel dynamic testing and analysis system is used for data collection and analysis in the experiment. The measured frequencies of the model car and the beam are shown in Table 5. The sampling frequency is 2 kHz. The data record time duration is 6 s. The model car has two axles at a space of 0·557 m and it runs on four rubber wheels. The mass of he whole car is 16·6 kg.

Figure 6 shows a sample of the measured strains at different locations. The first three modes are used in the identification. Correlation coefficients are calculated

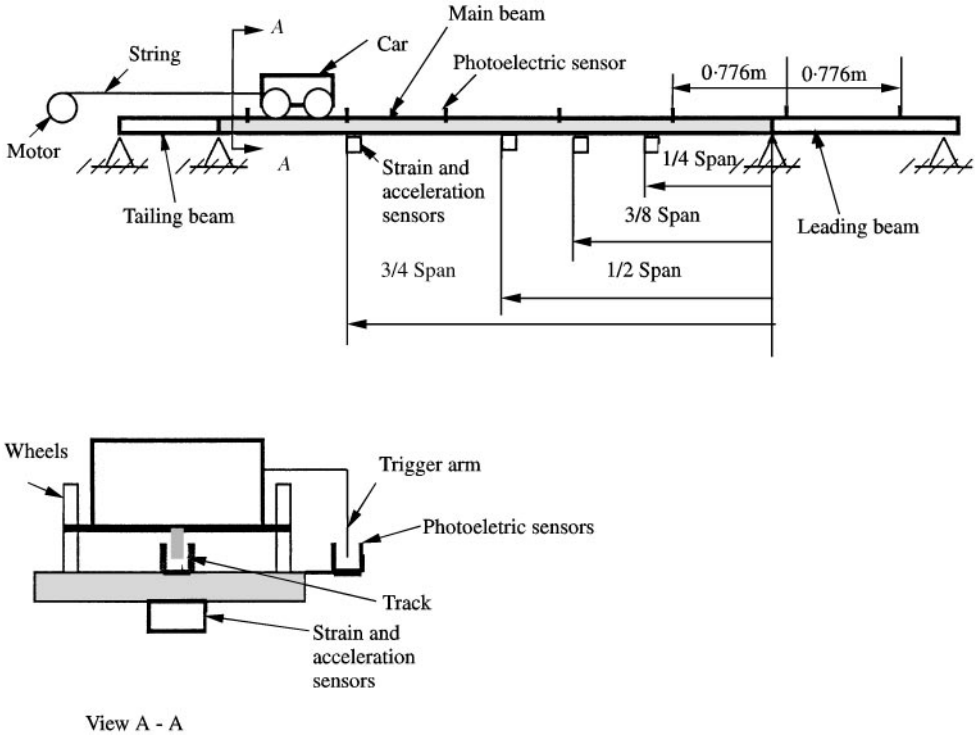

Figure 5. Diagrammatic drawing of experimental set-up.

TABLE 5

Natural frequencies of the model car and main beam

Mode	Model car (Hz)	Main beam (Hz)
1	7·82	3·67
2	9·77	16·83
3	11·72	37·83

between the reconstructed and measured responses, and they are shown in Table 6. Figures 7 and 8 show the identified results by using strains at $\frac{1}{4}$, $\frac{1}{2}$ and $\frac{3}{4}$ span. Figure 9 shows a comparison between the measured and the reconstructed strains at $\frac{3}{8}$ span by using the damping least-squares method (DLS) and by using the least–squares method (LS). The two identified forces are added together to become a resultant force as shown in Figure 10. The following conclusions are obtained from the experiments.

(1) Two impulses can be observed in the identified forces at around 0·6 and 3·3 s as shown in Figures 7, 8, and 10. These two moments correspond to the entry of the second axle and the exit of the first axle on the bridge deck, where the

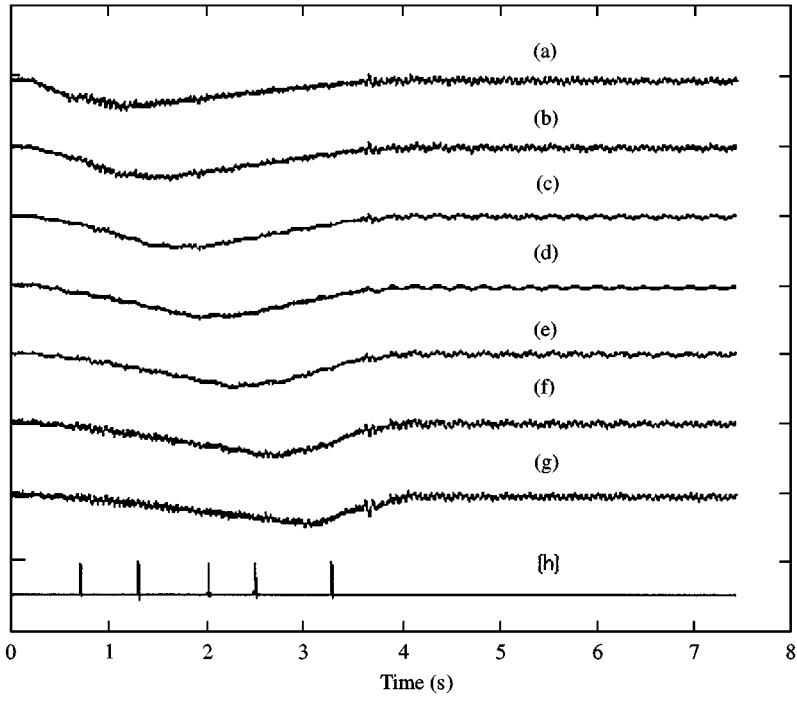

Figure 6. The recorded time histories from sensors in experiment.

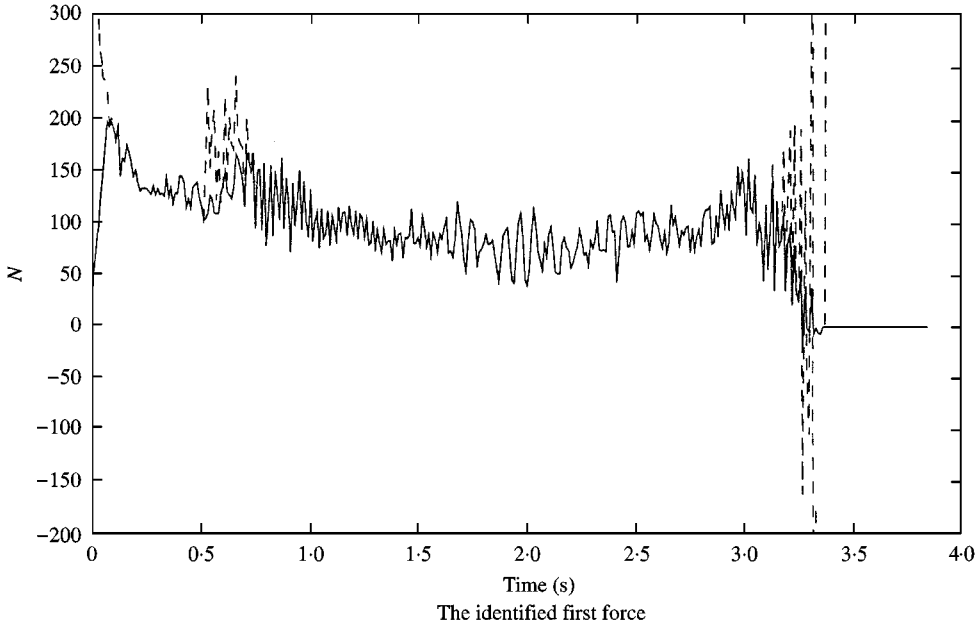

Figure 7. Time histories of identified first force in two forces experiment: ——, $\frac{1}{4}$, $\frac{1}{2}$, $\frac{2}{4}\varepsilon$ (DLS); - - - -, $\frac{1}{4}$, $\frac{1}{2}$, $\frac{3}{4}\varepsilon$ (LS).

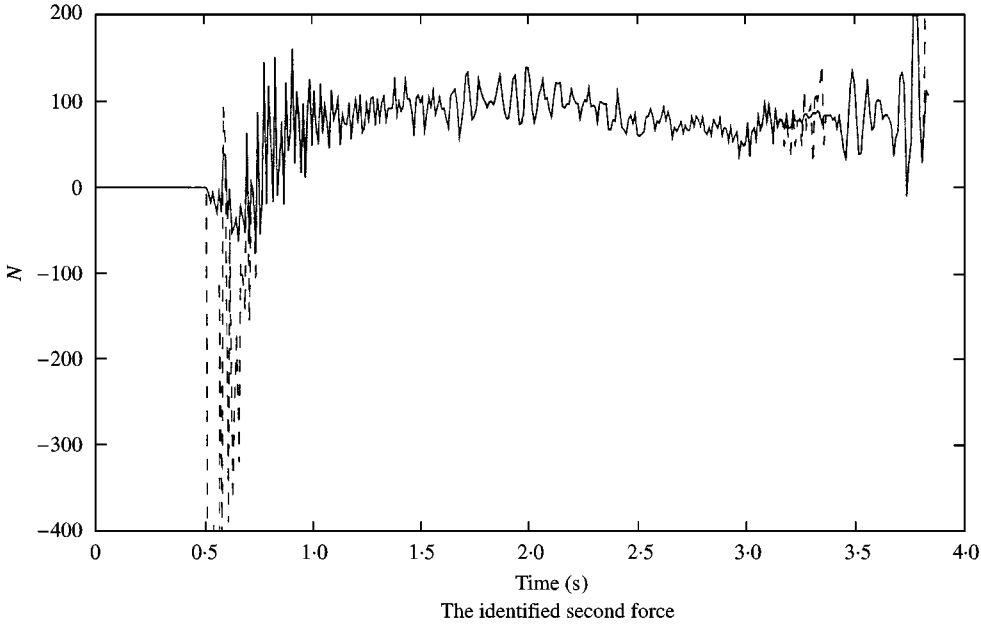

Figure 8. Time histories of identified second force in two forces experiment: ——, $\frac{1}{4}$, $\frac{1}{2}$, $\frac{3}{4}\varepsilon$ (DLS); - - - -, $\frac{1}{4}$, $\frac{1}{2}$, $\frac{3}{4}\varepsilon$ (LS).

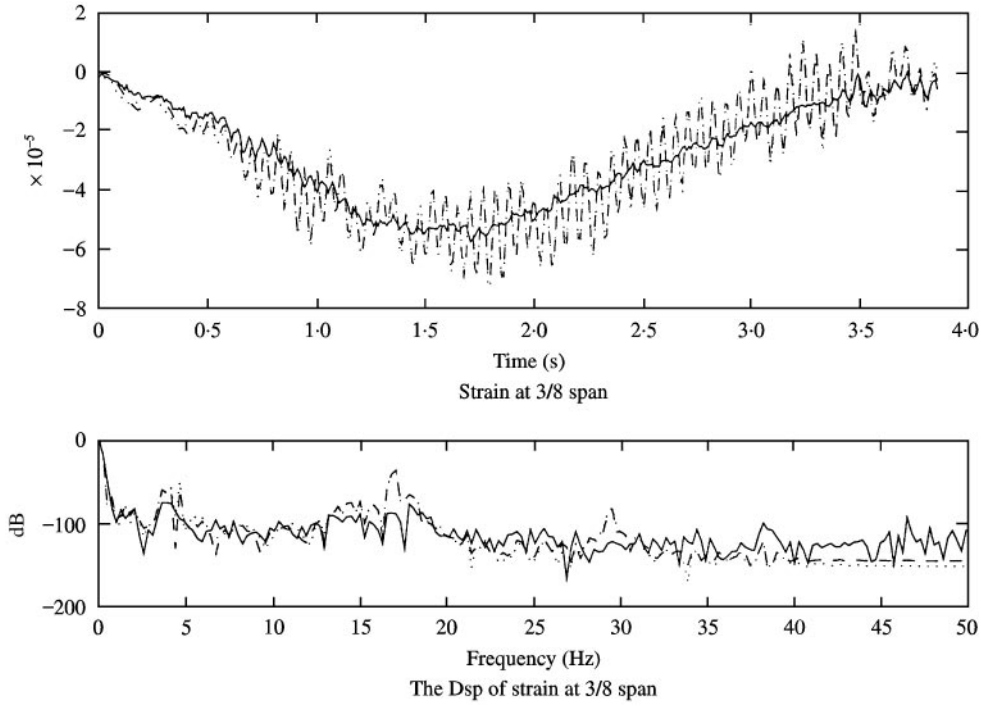

Figure 9. Comparison of measured and reconstructed strain at $\frac{3}{8}$ span: ——, measured response; - - - -, $\frac{1}{4}$, $\frac{1}{2}$, $\frac{3}{4}\varepsilon$ (DLS); ...., $\frac{1}{4}$, $\frac{1}{2}$, $\frac{3}{4}\varepsilon$ (LS).

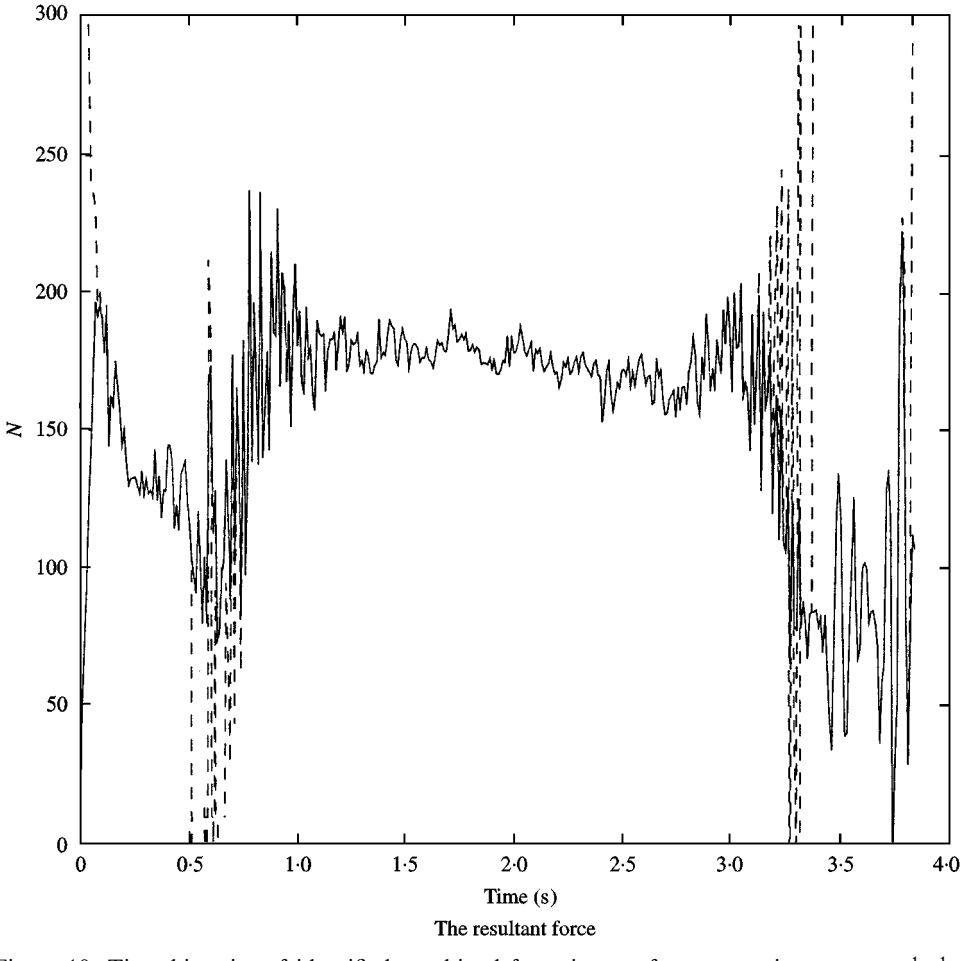

Figure 10. Time histories of identified combined force in two forces experiment: ——, $\frac{1}{4}$, $\frac{1}{2}$, $\frac{3}{4}\varepsilon$ (DLS); - - - -, $\frac{1}{4}$, $\frac{1}{2}$, $\frac{3}{4}\varepsilon$ (LS).

TABLE 6

Correlation coefficients between measured and calculated strain at $\frac{3}{8}$ span

Locations	DLS	LS
1/8a, 1/2s, 3/4s	0·9391	0·9335
1/4s, 1/2s, 3/4s	0·9391	0·9459
1/8s, 1/2s, 7/8s	0·9431	0·9352
1/8s, 1/4s, 1/2s	0·9189	0·6895
1/8s, 1/4s, 5/8s	0·9007	0·6736
1/8s, 1/4s, 7/8s	0·8936	0·6774
5/8s, 3/4s, 7/8s	0·7288	0·4356
1/8s, 1/4s, 3/4s, 5/8s	0·9294	0·9136
1/8s, 1/4s, 3/4s, 7/8s	0·8928	0·7576
1/8s, 1/4s, 1/2s, 3/4s, 7/8s	0·9459	0·9425
1/8s, 1/4s, 1/2s, 5/8s, 3/4s,7/8s	0·9407	0·9374
1/8s, 1/4s, 5/8s, 7/8s	0·9240	0·8976

forcing system switches from a single force excitation to a two-races excitation. They correspond to the points of discontinuation of the dependence between the forces and the responses.

(2) The results obtained from the damped least-squares method and the least-squares method are shown in Figures 7–10 and in Table 6 for comparison. The identified forces are almost identical in the middle length of the time duration. But when the forces are getting on and off the beam, large impulses are identified by the least-squares method but not by the damped least-squares method. The latter method is therefore more accurate and reliable in the identification.

(3) The reconstructed strains from the identified forces are close to the measured strain as shown in Figure 9. Almost all the correlation coefficients in Table 6 obtained from the DLS method larger than 0·89. These indicate that the proposed approach using DLS is effective in the force identification.

5. CONCLUSION

Computation simulations and laboratory tests show that:

(1) The proposed moving force identification method for a multi-span continuous non-uniform beam is effective, and acceptable results can be obtained.

(2) Computation simulations show that the error in the identified forces are acceptable when the number of measuring points is not less than the number of vibration modes.

(3) Both the strain and displacement measurements can be used in the moving force identification.

(4) The simulation and experimental results show that the damped least-squares method is better than the least-squares method in suppressing the unbounded ill-conditioned forces.

ACKNOWLEDGMENTS

The work described in this paper was supported by a grant from the Hong Kong Polytechnic University Research Funding Project No. V653. This work was carried out under the supervision of the second author.

REFERENCES

1. A. P. Whittemore, J. R. Wiley, P. C. Schultz and D. E. Pollock 1970 *Highway Research Board, National Cooperative Highway Research Program Report No.* 105. Dynamic pavement loads of heavy highway vehicles.
2. R. Cantieni 1992 *Swiss Federal Laboratories for Materials Testing and Research* (*EMPA*) *Report No.* 220. Dynamic behaviour of highway bridges under the passage of heavy vehicles.
3. S. S. Law, T. H. T. Chan and Q. H. Zeng 1997 *Journal of Sound and Vibration* **201**, 1–22. Moving force identification: a time domain method

4. S. S. Law, T. H. T. Chan and Q. H. Zeng 1999 *Journal of Dynamic Systems, Measurement and Control*, ASME. (In press). Moving force identification: a frequency and time domains methods.
5. T. H. T. Chan, S. S. Law, T. H. Yung and X. R. Yuan 1999 *Journal of Sound and Vibration* **219**, 503–524. An interpretive method for moving force identification.
6. S. S. Law and Y. L. Fang 1999 *Journal of Engineering Mechanics*, ASCE. Moving force identification: Optimal State Estimate Approach.
7. H. P. Lee 1994 *Journal of Sound and Vibration* **171**, 361–368. Dynamic response of a beam with intermediate point constraints subject to a moving load.
8. D. Y. Zheng, Y. K. Cheung, F. T. K. Au and Y. S. Cheng 1998 *Journal of Sound and Vibration* **212**, 455–467. Vibration of multi-span non-uniform beams under moving loads by using modified beam vibration functions.
9. J. S. Wu and C. W. Dai 1987 *Journal of Structural Engineering*, **113**, 458–474. Dynamic response of multi-span non-uniform beams due to moving loads.
10. K. Henchi and M. Fafard 1997 *Journal of Sound and Vibration* **199**, 33–50. Dynamic behaviour of multi-span beams under moving loads.
11. R. T. Wang 1997 *Journal of Sound and Vibration* **207**, 731–742. Vibration of multi-span Timoshenko beams to a moving force.
12. R. T. Wang and J. S. Lin 1998 *Structural Engineering and Mechanic* **6**, 229–243. Vibration of T-type Timoshenko frames subjected to moving loads.
13. D. C. Kammer 1998 *Journal of Vibration and Accoustics* **120**, 868–874. Input force reconstruction using a time domain technique.
14. T. C. Huang 1961 *Journal of Applied Mechanics* **28**, 578–584. The effect of rotatory inertial and of shear deformation on the frequency and normal mode equations of uniform beams with simple and conditions.
15. A. M. Tikhonov 1963 *Soviet Mathematics* **4**, 1035–1038. On the solution of ill-posed problems and the method of regularization.
16. C. W. Groetsch 1993 '*Inverse Problems in the Mathematical Sciences*'. Vieweg.
17. G. H. Golub and M. Heath 1979 *Technometrics* **21**, 215–223. Generalized cross-validation as a method for choosing a good ridge parameter.
18. J. C. Santantamarina and D. Fratta 1998 *Introduction to Discrete Signals and Inverse Problems in Civil Engineering*, 200–238. ASCE Press.

APPENDIX: NOMENCLATURE

$A(x)$	area of cross-section
c_{ij}	generalized damping
$EI(x)$	flexural stiffness of beam
$f_i(t)$	ith generalized force
$\mathbf{F}$	generalized force matrix
G	shear modulus
k	stiffness of point constraint
k_{ij}	generalized stiffness
$\mathbf{K}$	generalized stiffness matrix
m_{ij}	generalized mass
$\mathbf{M}$	generalized mass matrix
$P_i(t)$	ith moving load
$q_i(t)$	ith generalized co-ordinate
T	kinetic energy
U_e	bending energy of beam
U_Q	potential energy due to point constraints
$v(t)$	speed of moving load
W	work done by the moving loads

x_i	initial position of ith moving load
x_l	location of measurement location
$y(x, t)$	displacement function of beam
$Y_i(x_s)$, $\phi_i(x)$	assumed displacement mode shapes
$\gamma(x)$	radius of gyration of cross-section
$\delta(t)$	Dirac delta function
$\varepsilon(x_s, t)$	measured strain at location x_s
κ	shear coefficient
λ	non-negative damping coefficient
$\psi(x, t)$	angle of rotation of cross-section
$\|\cdot\|$	norm of a vector of matrix